Langmuir

Article

pubs.acs.org/Langmuir

Sol–Gel-Derived Silver-Nanoparticle-Embedded Thin Film for Mass Spectrometry-Based Biosensing

Roberto C. Gamez, Edward T. Castellana, and David H. Russell*

Department of Chemistry, Laboratory for Biological Mass Spectrometry, Texas A&M University, College Station, Texas 77843, United States

Supporting Information

ABSTRACT: A porous silver-nanoparticle (AgNP)-embedded thin film biosensor was produced by the sol–gel method. The thin films were used as matrix-free laser desorption ionization mass spectrometry (LDI-MS) biosensors applicable to several chemical classes. In these experiments, UV laser irradiation (337 nm) of the AgNP facilitates desorption and ionization of a number of peptides, triglycerides, and phospholipids. Preferential ionization of sterols from vesicles composed of olefinic phosphosphatidylcholines is also demonstrated, offering the possibility for a simplified approach for sterol analysis from complex mixtures. The composition of the nanoparticles was confirmed by X-ray photoelectron spectroscopy (XPS) and UV–vis spectroscopy. XPS data revealed a binding energy of 368.2 eV, consistent with the previous assignment of the binding energy for the Ag $3d_{5/2}$ peak from Ag^0 at 368.1 ± 0.1 eV. The surface morphology of the thin films was studied by field-emission scanning electron microscopy (FE-SEM) and revealed the presence of nanoparticles and the porous nature of the biosensor.

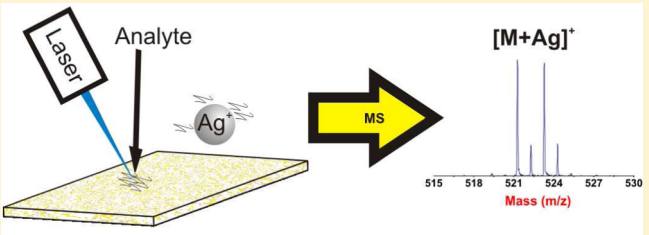

INTRODUCTION

Owing to their biological significance, the rapid detection of peptides, proteins, and lipids has become the basis for the development of numerous biosensing techniques over the past several years. Among these techniques, matrix-assisted laser desorption ionization mass spectrometry (MALDI-MS) has been proven to be invaluable for the analysis of a number of high-molecular-weight compounds;[1−4] however, its utility in the analysis of small molecules (<1000 m/z) such as steroids and lipids has been limited by significant background noise from matrix clusters that congest the low-mass region of the spectra.[5,6] A number of matrix-free platforms have since been developed to probe lower-mass-region analytes with considerable success. One such method, desorption ionization on porous silicon (DIOS), utilizes etched silicon wafers to fabricate a porous nanostructure that can be used for directly desorbing and ionizing analytes from the surface.[7−10] Although this method has been proven successful in both minimizing background noise and detecting several low-molecular-weight compounds including peptides and organic compounds, the technique has been generally limited to basic analytes.[11] Additionally, the shelf life of the DIOS platform is relatively short owing to its susceptibility to surface oxidation, which results in decreased performance and reproducibility.[10,11]

Alternatively, the sol–gel method has recently gained considerable attention as a simple means for producing effective MS platforms via the incorporation of organic matrices and optically active metal nanoparticles (NPs) that serve as UV energy absorbers. Separate studies utilizing thin films impregnated with α-cyano-4-hydroxycinnamic acid (CHCA) and 2,5-dihydroxybenzoic acid (DHB) were capable of detecting a number of small molecules and proteins, respectively.[12,13] Several oligonucleotides were successfully analyzed by doping 3,4-diaminobenzoic acid (DABA) or 3,5-DABA into sol–gel solutions during the preparation of thin films, a method that also proved to be effective in reducing interference signals associated with alkali metal salts without desalting steps prior to analysis.[14] Incorporating TiO_2 into the sol–gel allowed for the detection of surfactants, peptides, and tryptic digest products; however, the addition of a proton source in the form of citrate buffer was necessary for useful MS data.[15]

There are distinct advantages of the sol–gel method for the synthesis of metal NPs compared to traditional chemical reduction methods. Namely, organometallic precursors such as metal salts are often miscible with the starting solution, and controlled homogeneous doping is easily achieved. Moreover, because high annealing temperatures are oftentimes employed, low-mass organic residuals that may potentially interfere in MS analysis are incinerated during the process, thereby eliminating additional cleanup steps.[16,17] Here, we describe the preparation and implementation of a porous AgNP-embedded thin film platform prepared using standard sol–gel chemistry to form an optically active LDI-MS biosensor platform. The AgNP/thin film serves as an alternative matrix-free MS platform for the sensitive detection of a number of low-abundance sterols from

Received: March 7, 2013
Revised: April 22, 2013

 © XXXX American Chemical Society dx.doi.org/10.1021/la4008526 | Langmuir XXXX, XXX, XXX–XXX

lipid vesicles as well as several analytes in various chemical classes. The combination of optically active NP with the high concentration of pores on the film surface provides several advantages from an analytical standpoint, including (i) increased sample loading offered by the larger surface area of the system, (ii) minimized sample preparation, (iii) a high tolerance to salts by the elimination of chemical stabilizers, and (iv) an extended shelf life (>1 year).

EXPERIMENTAL SECTION

Materials. All peptides (Angiotensin I, Angiotensin II, Angiotensin III, [Val^4] Angiotensin III, Bradykinin, Substance P, etc.) were purchased from American Peptide Co., Inc. (Sunnyvale, CA). 1,2-Dioleoyl-*sn*-glycero-3-phosphocholine (DOPC), 1-palmitoyl-2-oleoyl-*sn*-glycero-3-phosphocholine (POPC), 1,2-dipalmitoyl-*sn*-glycero-3-phosphocholine (DPPC), and 1,2-dimyristoyl-*sn*-glycero-3-phosphocholine (DMPC) were acquired from Avanti Polar Lipids (Alabaster, AL). Triglyceride standard mixture, tetraethyl orthosilicate (TEOS), 2-ethoxyethanol, and silver nitrate were purchased from Sigma-Aldrich, Inc. (St. Louis, MO). All aqueous solutions were prepared using 18.2 MΩ/cm^2 water (Barnstead EasyPure II, Thermo Scientific, Dubuque, IA). Boro-aluminosilicate glass wafers, (25.4 × 25.4 mm^2, 0.5 mm thick) were purchased from Precision Glass & Optics (Santa Ana, CA). Glass wafers were cleaned by immersion in piranha solution (75% concentrated sulfuric acid, 25% concentrated hydrogen peroxide) at 100 °C for 30 min. ***Caution!*** *Piranha solution is a vigorous oxidant and should be used with extreme caution.* Next, the wafers were rinsed thoroughly with water and baked at 150 °C for 2 h prior to use.

Sol–Gel Thin Film Preparation. Porous AgNP-impregnated thin films were prepared by the sol–gel method. First, 15.9 mL of TEOS, 15.3 mL of 2-ethoxyethanol, and 4.8 mL of distilled water were mixed at room temperature with stirring. Next, 0.5 mL of 0.5 M nitric acid was added to the mixture to make the pH of the solution acidic. This solution was stirred at room temperature for 4 h, and then 1.46 g of silver nitrate was added and the mixture was allowed to stir for an additional 2 h. After stirring, the clean glass wafers were coated with the silver-containing sol–gel solution by a spin-coating process. Individual glass slides were placed on the spin-coating platform, and the surfaces were subjected to 4 mL of silver-containing sol–gel solution while spinning at 1200 rpm for 30 s. The freshly coated wafers were then thermally treated in a furnace in air. The furnace was ramped from room temperature to 700 °C over 7 h and held at 700 °C for 3 h, followed by a ramp down to room temperature over 7 h. The thermally treated films were stored under atmospheric conditions and used without further treatment.

Instrumentation. Mass spectrometry data were acquired with a Voyager DE-STR MALDI-TOF-MS (Applied Biosystems, Foster City, CA). UV-LDI-MS (337 nm) was carried out using a nitrogen laser (model VSL-337ND-S, Thermo Laser Science, Franklin, MA).

Characterization. UV–vis absorption spectra of the thin films were acquired with an Agilent 8453 spectrophotometer. SEM images were acquired with a FEI Quanta 600 FE-SEM, and pore size distributions were determined directly from the SEM images using ImageJ particle size analysis software. X-ray photoelectron spectroscopy (XPS) measurements were carried out using a Kratos Axis Ultra Imaging X-ray photoelectron spectrometer. A monochromated Al Kα source of $h\nu$ = 1486.6 eV was used to probe the thin films. Binding energies were corrected by C 1s as a reference energy (C 1s = 248.8 eV).[18] Narrow scans of the Ag 3d regions were collected at an analyzer pass energy of 40 eV after five scan repetitions with a measuring step of 0.1 eV and a dwell time of 450 ms.

METHODS

Thin films were taped directly to the surface of a standard stainless steel MALDI plate with copper tape. Analyzed samples (1.0 μL) were spotted directly on the surface of the AgNP-impregnated films. Data acquisition was performed on a Voyager DE-STR equipped with a nitrogen laser (337 nm) in reflection mode. Laser intensities were adjusted to optimize the signal-to-noise ratio, and desorbed ions were extracted into the flight tube with 20 kV after a 200 ns delay. Laser energies used for signal production ranged from ~3.5 to 6.0 μJ/pulse, and laser energy measurements were acquired using an Ophir Nova Power/Energy meter coupled to a PE-10 Ophir pyroelectric head (Ophir Laser Measurement Group, North Logan, UT). Values were recorded every 200 shots from a total of 1000 laser shots, and measurements were taken in increments of 50 arbitrary units via the instrument control settings.

RESULTS AND DISCUSSION

The utility of AgNP-impregnated thin films as a platform for mass spectrometry analysis is demonstrated for a number of analytes that were individually spotted directly onto the surface and vacuum-dried. LDI-MS analysis was performed by irradiation of each sample spot with 337 nm photons. It should be emphasized that LDI was carried out without the addition of organic matrices. We hypothesize that the overlap of the SPR band of the AgNP is capable of absorbing the incoming laser radiation that results in (i) a rapid rise in temperature of the nanoparticles,[19] which facilitates the thermal desorption of the analyte and (ii) the production of silver ions[20] that ionize the samples spotted on the surface. LDI yields primarily silver ion clusters, and the analytes are typically observed as Ag$^+$ adducts that have a characteristic isotopic pattern consisting of two dominant peaks with an approximate 1:1 intensity ratio separated by 2 m/z units. The data in Figure 1 demonstrate the capability of the thin films to produce signals

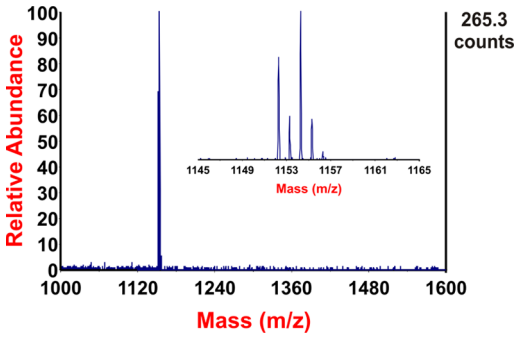

Figure 1. Mass spectrum of 2.5 pmol Angiotensin II (m/z = 1152.5) spotted on a AgNP thin film surface and analyzed by LDI-MS. (Inset) Closeup view of the resulting peak.

when 2.5 pmol of Angiotensin II (DRVYIHPF) is spotted on the surface and analyzed. Here, the only signal observed corresponds to a silver adduct of the peptide, [Angiotensin II + Ag]$^+$ (m/z = 1152.4). The inset of Figure 1 shows the unique isotope pattern of the silver adducted analyte. Moreover, the spectrum shows minimal background noise and a high signal-to-noise ratio (s/n ≈ 250). Similar results were observed for a number of analytes, and the results are summarized in the Supporting Information (Figure S1).

The versatility of AgNP thin films as a mass spectrometry platform was evaluated by analyzing a mixture of triglycerides (TAG, C8–C16) and phosphatidylcholines (DMPC, DPPC, and POPC). The analytes in the mixture contain saturated hydrocarbon chain moieties except for POPC, which has a single site of unsaturation in one of the hydrocarbon chains. As previously mentioned, the thin film was left untreated and the mixture was spotted directly onto the surface, dried, and analyzed. The resulting mass spectrum (Figure 2) contains [M

dx.doi.org/10.1021/la4008526 | Langmuir XXXX, XXX, XXX–XXX

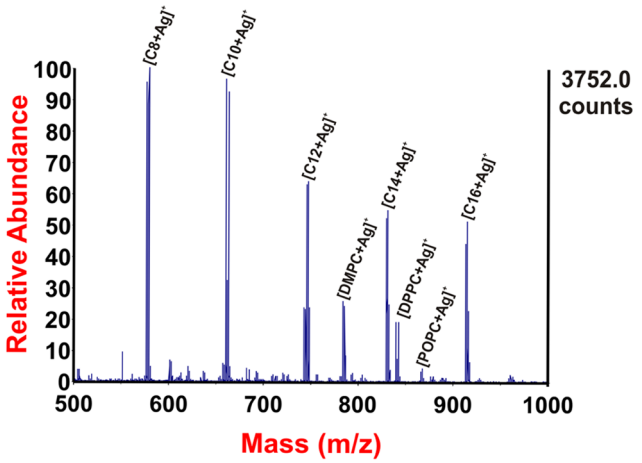

	Chain Length	[M+Ag]+	Counts	pmol spotted
TAG	8:0	577.3	3752.0	10.6
TAG	10:0	661.4	3623.9	9.01
TAG	12:0	745.5	2394.7	7.82
TAG	14:0	829.5	2058.1	6.91
TAG	16:0	913.6	1920.8	6.19
DMPC	PC(14:0/14:0)	784.4	972.9	7.37
DPPC	PC(16:0/16:0)	840.5	723.4	6.81
POPC	PC(16:0/18:1)	866.5	179.2	6.58

Figure 2. Mass spectrum of a mixture containing a triglyceride mixture and three phosphatidylcholines (DMPC, DPPC, and POPC) analyzed by LDI-MS. The table lists the amount spotted on the surface and the corresponding counts produced.

+ Ag]$^+$ signals for each of the TAGs and phospholipids in the mixture. Interestingly, POPC, the only olefin present in the mixture, produced the lowest ion abundance despite being spotted at a concentration (~6 pmol) equal to that of the other analytes. This observation is consistent with our previous investigation in which we attributed the lower ionization efficiency of POPC to a weaker interaction between the silver ions and the double bond owing to the steric hindrance imposed on the silver ion by the freely rotating long hydrocarbon chains.[21,22] Similar results were obtained for small unilamellar vesicles composed of different sterols and phosphatidylcholines with either one or two unsaturated tails. In these experiments, the vesicles prepared were composed of ~99.5 mol % POPC and ~0.5 mol % stigmasterol, lanosterol, β-sitosterin, or cholecalciferol. For each of the preparations containing the olefins, preferential ionization of the sterols is observed, and the dominant peak in each of the resulting spectra corresponds to the Ag$^+$ adduct of the sterol. Figure 3 contains a typical spectrum for the analysis of the sterol/unsaturated lipid vesicle mixture. For this analysis, the vesicles were diluted such that ~2 pmol of stigmasterol and ~330 pmol of POPC were spotted onto the surface. Despite the lower concentration of sterols compared to that of the phospholipids, the dominant signal corresponds to each of the individual sterols for the respective analyses. It should be noted that the sterols were also preferentially ionized from preparations using DOPC lipid vesicles (data not shown).

Minimizing sample handling that might lead to sample loss is essential for the successful detection of target molecules in the analysis of complex mixtures. This is especially true in the case of biological fluids that require cleanup steps to reduce the high

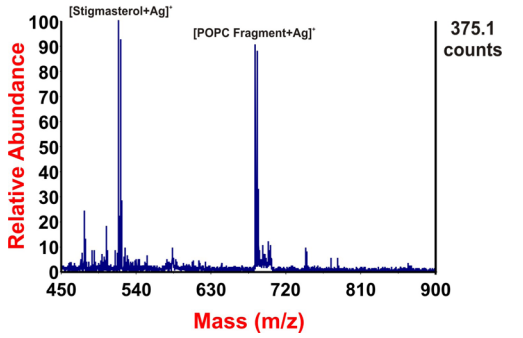

Figure 3. Mass spectrum of vesicles composed of 99.5 mol % POPC and 0.5 mol % stigmasterol. The vesicles were diluted so that ~2 pmol of stigmasterol and ~330 pmol of POPC were spotted onto the surface. The POPC fragment corresponds to the loss of the phosphatidylcholine headgroup.

salt concentrations that frequently complicate mass spectrometry analysis owing to the formation of salt adducts or the production of chemical background noise. Figure 4 contains

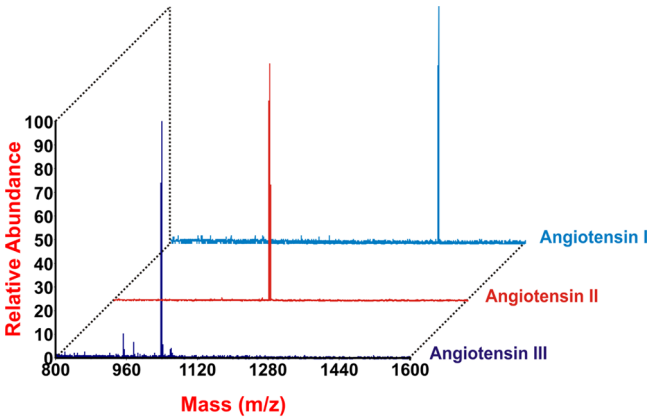

	Sequence	[M+Ag]+	Counts	pmol spotted
Angiotensin I	DRVYIHPFHL	1402.6	236.2	7.71
Angiotensin II	DRVYIHPF	1152.4	1069.5	9.55
Angiotensin III	RVYIHPF	1037.4	381.1	10.7

Figure 4. Mass spectra of Angiotensin I–III when diluted in 1.0 mM NaCl and analyzed by LDI-MS. The table lists the amount in picomoles spotted for the analysis and the corresponding counts produced for each of the analytes.

mass spectra produced when three analytes were diluted to their final concentrations in 1 mM NaCl and analyzed using the AgNP thin films. Although the analytes are present at concentrations of ~10 pmol under high salt conditions, the dominant signal in each of the individual spectra corresponds to [M + Ag]$^+$ rather than [M + Na]$^+$ for the respective analytes with little to no background noise or interference peaks. The concentrations for each of the analytes and the corresponding counts at those concentrations are summarized in the figure. Similar results were observed for a number of other biological buffers including 1.0 mM urea, 1.0 mM ammonium acetate, and Tris-buffered saline (1.0 mM Tris/3.0 mM NaCl) (Figures S2–S4, Supporting Information). Additionally, these results were acquired from the surface of a platform that had been prepared 16 months prior to the analysis (platform prepared December 2011; data taken April 2013).

During the course of developing the technology, AgNP-embedded sol–gels were stored under atmospheric conditions

dx.doi.org/10.1021/la4008526 | Langmuir XXXX, XXX, XXX–XXX

for periods >1 year. Lengthy storage periods did not compromise the functionality of the platform. For example, the feasibility of preparing the thin films for future use as a durable analysis platform is demonstrated by the low-mass region of a mass spectrum (data taken December 2011) of an unspotted thin film prepared in September of 2010 (Figure S5, Supporting Information). The film is still capable of producing an abundance of silver ions, which can be used to ionize analytes spotted on the surface a year after initial preparation, despite remaining under atmospheric conditions. In fact, when several different analytes were spotted on the surface of an aged film, abundant signal for 2.5 pmol of analyte spotted onto the surface could still be produced (Figures S6–S8, Supporting Information). It should be noted that the low-mass region does contain additional unidentified interference peaks; however, the higher-mass region where analyte signal is produced remains relatively unchanged and analyte identification is easily achieved.

After thermal treatment at 700 °C, the resulting AgNP thin film has a distinct yellow color (Figure 5) that remains unchanged for a period of several months despite being stored under atmospheric conditions. The optical absorption spectrum of the silver-doped thin film displays a strong absorption band centered at ~390 nm that is attributed to the surface plasmon resonance (SPR) of the AgNP in the film.[23] The optical absorption of several regions of the films showed minimum variability in the optical properties across the platform (Figure S9, Supporting Information). As evident from an overlay of the optical spectra of fresh and aged films shown in Figure 5, long storage periods under ambient conditions did not appear to alter the optical properties of the film significantly. The surface morphology of the thin films was examined by scanning electron microscopy (SEM), which revealed the porous nature of the film and the presence of AgNP on the surface (Figure S10, Supporting Information). The average pore size distribution was determined to be ~650 nm in diameter, which remained consistent across individual thin film preparations (Figure S11, Supporting Information).

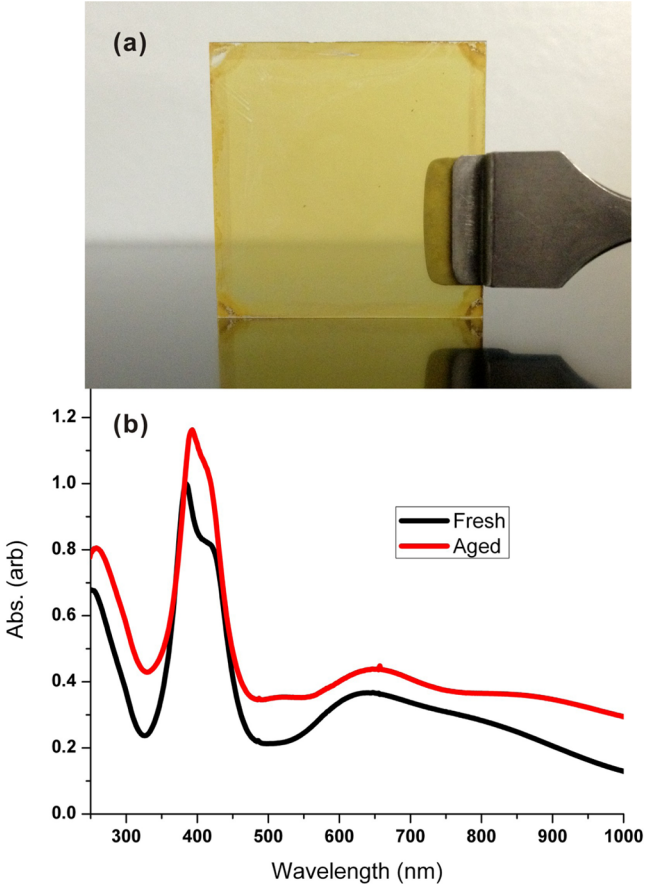

Figure 5. (a) Resulting thin film after spin coating and thermal treatment. (b) Optical absorption spectra of fresh and aged (>1 year) AgNP thin films. Note that the spectrum of the aged film is offset by 0.2 Abs for clarity.

Although the mechanism governing the formation of the AgNPs is not yet entirely understood, there have been several investigations focused on the production and characterization of Ag-doped films utilizing the sol–gel method.[24−27] In these studies, it was discovered that the reduction of Ag^+ is achieved only at temperatures above 500 °C and that lower annealing temperatures do not yield nanoparticles. Epifani et al. suggested that the reduction of Ag^+ to Ag^0 is inhibited by the formation of silver complexes, and reduction can be achieved only by the thermal decomposition of the complexes. This conclusion was supported by the fact that heating at lower temperatures (300 °C) produced no detectable optical absorption corresponding to the SPR band for AgNPs; a similar result was obtained when lower heating temperatures were used in our method of preparation (Figure S12, Supporting Information). Previously, Weaver and Hoflund studied the thermal decomposition of Ag_2O by X-ray photoelectron spectroscopy (XPS) and discovered that annealing at a temperature of 490 °C for 60 min was sufficient to reduce the bulk of the Ag_2O sample to Ag metal.[28] In our experiments, the formation of AgNP is further supported by XPS measurements of the films. Ag metal, AgO, and Ag_2O powder have been studied extensively by XPS, and it has been established that an increase in the oxidation state of silver results in a negative shift of the binding energy of Ag 3d peaks.[28−31] Figure 6 shows the Ag 3d core-level spectrum of the Ag thin film that exhibits an expected Ag 3d doublet. The peak at a binding energy of 368.2 eV is consistent with the previous assignment of the binding energy for the Ag $3d_{5/2}$ peak from Ag^0 at 368.1 ± 0.1 eV.[32] It should be noted that the best signal

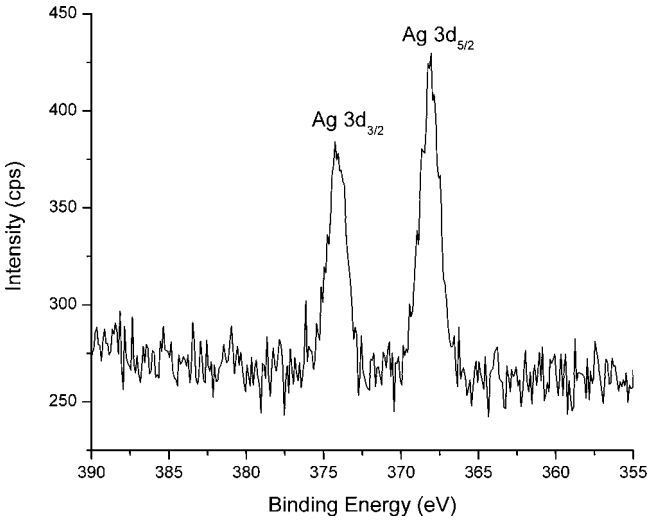

Figure 6. The Ag 3d binding energy XPS spectrum of a silver thin film. The resulting peaks indicate that silver exists in the elemental form.

dx.doi.org/10.1021/la4008526 | Langmuir XXXX, XXX, XXX–XXX

for the XPS experiments was obtained when the surface of the film was scratched just prior to analysis, leading us to hypothesize that AgNPs are not only at the surface of the film but also embedded within the SiO_2 matrix as well.

In our method, the thin films were heated to a final temperature of 700 °C to ensure the formation of AgNP and the decomposition of residual organics that can complicate the spectra during mass spectrometric analysis. The fact that there are few low mass interference peaks when the surface is interrogated by LDI-MS manifests the decomposition of organics. Additionally, the higher temperature also allows for the freshly prepared AgNP films to be used without any additional handling steps such as washing or surface treatment after initial preparation.

CONCLUSIONS

A porous AgNP-impregnated thin film prepared by a sol−gel method is demonstrated as a flexible platform for LDI-MS of analytes of various chemical classes. The AgNP-impregnated thin film absorbs incoming photons, resulting in desorption and ionization of analytes, which are observed as Ag^+ adducts. This investigation focuses on the analysis of several nonolefin analytes, specifically, peptides and several phospholipids/triglycerides with fully saturated hydrocarbon tails. Possibly of greater interest is the preferential ionization of sterols from vesicles composed primarily of olefinic phosphosphatidylcholines, which offers the possibility of a simplified approach to sterol analysis from mixtures. Moreover, the platform displayed an excellent shelf life and retained its optical properties for over a year without compromising LDI-MS function, an appealing quality from a diagnostic standpoint where minimal sample preparation is often required for rapid analysis. Alternative plasmonic nanoparticles such as Cu(II) and Fe(III) for selective ionization are currently being investigated. Additionally, tailoring the surface chemistry of the platform through biofunctionalization techniques involving silane chemistry for added selectivity is also being explored.

ASSOCIATED CONTENT

Supporting Information

Analytes table, mass spectra of peptides diluted in biological buffers from aged films, SEM image of the surface, and optical spectra including different regions of the thin films. This material is available free of charge via the Internet at http://pubs.acs.org

AUTHOR INFORMATION

Corresponding Author

*E-mail: russell@chem.tamu.edu. Phone: (979) 845-3345.

Notes

The authors declare no competing financial interest.

ACKNOWLEDGMENTS

The metal nanoparticle synthesis and preparation research was funded by The Robert A. Welch Foundation (A-1176). The laser desorption ionization and biosensor development research was funded by the U. S. Department of Energy, Division of Chemical Sciences, BES(DE-FG02-04ER15520).

REFERENCES

(1) Karas, M.; Hillenkamp, F. Laser Desorption Ionization of Proteins with Molecular Masses Exceeding 10000 Da. *Anal. Chem.* **1988**, *60*, 2299−2301.

(2) Karas, M.; Bahr, U. Laser Desorption Ionization Mass-Spectrometry of Large Biomolecules. *TrAC, Trends Anal. Chem.* **1990**, *9*, 321−325.

(3) Strupat, K.; Karas, M.; Hillenkamp, F. 2,5-Dihydroxybenzoic Acid - A New Matrix for Laser Desorption Ionization Mass-Spectrometry. *Int. J. Mass Spectrom. Ion Process.* **1991**, *111*, 89−102.

(4) Karas, M.; Bahr, U.; Ingendoh, A.; Hillenkamp, F. Laser Desorption Ionization Mass-Spectrometry of Proteins of Mass 100 000 to 250 000 Da. *Angew. Chem., Int. Ed. Engl.* **1989**, *28*, 760−761.

(5) Peterson, D. S. Matrix-Free Methods for Laser Desorption/Ionization Mass Spectrometry. *Mass Spectrom. Rev.* **2007**, *26*, 19−34.

(6) Cohen, L. H.; Gusev, A. I. Small Molecule Analysis by MALDI Mass Spectrometry. *Anal. Bioanal. Chem.* **2002**, *373*, 571−586.

(7) Thomas, J. J.; Shen, Z. X.; Crowell, J. E.; Finn, M. G.; Siuzdak, G. Desorption/Ionization on Silicon (DIOS): A Diverse Mass Spectrometry Platform for Protein Characterization. *Proc. Natl. Acad. Sci. U.S.A.* **2001**, *98*, 4932−4937.

(8) Lewis, W. G.; Shen, Z. X.; Finn, M. G.; Siuzdak, G. Desorption/Ionization on Silicon (DIOS) Mass Spectrometry: Background and Applications. *Int. J. Mass Spectrom.* **2003**, *226*, 107−116.

(9) Wei, J.; Buriak, J. M.; Siuzdak, G. Desorption-Ionization Mass Spectrometry on Porous Silicon. *Nature* **1999**, *399*, 243−246.

(10) Shen, Z. X.; Thomas, J. J.; Averbuj, C.; Broo, K. M.; Engelhard, M.; Crowell, J. E.; Finn, M. G.; Siuzdak, G. Porous Silicon as a Versatile Platform for Laser Desorption/Ionization Mass Spectrometry. *Anal. Chem.* **2001**, *73*, 612−619.

(11) Ostman, P.; Pakarinen, J. M. H.; Vainiotalo, P.; Franssila, S.; Kostiainen, R.; Kotiaho, T. Minimum Proton Affinity for Efficient Ionization with Atmospheric Pressure Desorption/Ionization on Silicon Mass Spectrometry. *Rapid Commun. Mass Spectrom.* **2006**, *20*, 3669−3673.

(12) Laughlin, J. B.; Cassady, C. J.; Cox, J. A. Matrix-Assisted Laser Desorption Ionization of Small Biomolecules Impregnated in Silica Prepared by a Sol-Gel Process. *Rapid Commun. Mass Spectrom.* **1997**, *11*, 1505−1508.

(13) Lin, Y. S.; Chen, Y. C. Laser Desorption/Ionization Time-of-Flight Mass Spectrometry on Sol-Gel-Derived 2,5-Dihydroxybenzoic Acid Film. *Anal. Chem.* **2002**, *74*, 5793−5798.

(14) Chen, W. Y.; Chen, Y. C. Reducing the Alkali Cation Adductions of Oligonucleotides Using Sol-Gel-Assisted Laser Desorptionionization Mass Spectrometry. *Anal. Chem.* **2003**, *75*, 4223−4228.

(15) Chen, C. T.; Chen, Y. C. Molecularly Imprinted TiO_2-Matrix-Assisted Laser Desorption/Ionization Mass Spectrometry for Selectively Detecting α-Cyclodextrin. *Anal. Chem.* **2004**, *76*, 1453−1457.

(16) Pierre, A. C.; Pajonk, G. M. Chemistry of Aerogels and Their Applications. *Chem. Rev.* **2002**, *102*, 4243−4265.

(17) Gurav, J. L.; Jung, I. K.; Park, H. H.; Kang, E. S.; Nadargi, D. Y. Silica Aerogel: Synthesis and Applications. *J. Nanomater.* **2010**, *2010*, 1−11.

(18) Moulder, J. F. S., W. F.; Sobol, P. E.; Bomben, K. D. *Handbook of X-ray Photoelectron Spectroscopy*; Perkin-Elmer: Eden Prarie, MN, 1992.

(19) Link, S.; El-Sayed, M. A. Spectral Properties and Relaxation Dynamics of Surface Plasmon Electronic Oscillations in Gold and Silver Nanodots and Nanorods. *J. Phys. Chem. B* **1999**, *103*, 8410−8426.

(20) Kamat, P. V.; Flumiani, M.; Hartland, G. V. Picosecond Dynamics of Silver Nanoclusters. Photoejection of Electrons and Fragmentation. *J. Phys. Chem. B* **1998**, *102*, 3123−3128.

(21) Sherrod, S. D.; Diaz, A. J.; Russell, W. K.; Cremer, P. S.; Russell, D. H. Silver Nanoparticles As Selective Ionization Probes for Analysis of Olefins by Mass Spectrometry. *Anal. Chem.* **2008**, *80*, 6796−6799.

(22) Dewar, J. S. A Review of the π-Complex Theory. *Bull. Soc. Chim. Fr.* **1951**, *18*, C71−C79.
(23) Kreibig, U.; Vollmer, M. *Optical Properties of Metal Clusters*; Springer: Berlin, 1995.
(24) Jeon, H. J.; Yi, S. C.; Oh, S. G. Preparation and Antibacterial Effects of Ag-SiO_2 Thin Films by Sol-Gel Method. *Biomaterials* **2003**, *24*, 4921−4928.
(25) Epifani, M.; Giannini, C.; Tapfer, L.; Vasanelli, L. Sol-Gel Synthesis and Characterization of Ag and Au Nanoparticles in SiO_2, TiO_2, and ZrO_2 Thin Films. *J. Am. Ceram. Soc.* **2000**, *83*, 2385−2393.
(26) Mennig, M.; Schmitt, M.; Schmidt, H. Synthesis of Ag-Colloids in Sol-Gel Derived SiO_2-Coatings on Glass. *J. Sol-Gel Sci. Technol.* **1997**, *8*, 1035−1042.
(27) De, G.; Licciulli, A.; Massaro, C.; Tapfer, L.; Catalano, M.; Battaglin, G.; Meneghini, C.; Mazzoldi, P. Silver Nanocrystals in Silica by Sol-Gel Processing. *J. Non-Cryst. Solids* **1996**, *194*, 225−234.
(28) Weaver, J. F.; Hoflund, G. B. Surface Characterization Study of the Thermal-Decomposition of Ag_2O. *Chem. Mater.* **1994**, *6*, 1693−1699.
(29) Weaver, J. F.; Hoflund, G. B. Surface Characterization Study of the Thermal-Decomposition of AgO. *J. Phys. Chem.* **1994**, *98*, 8519−8524.
(30) Kaspar, T. C.; Droubay, T.; Chambers, S. A.; Bagus, P. S. Spectroscopic Evidence for Ag(III) in Highly Oxidized Silver Films by X-ray Photoelectron Spectroscopy. *J. Phys. Chem. C* **2010**, *114*, 21562−21571.
(31) Hoflund, G. B.; Hazos, Z. F.; Salaita, G. N. Surface Characterization Study of Ag, AgO, and Ag_2O Using X-ray Photoelectron Spectroscopy and Electron Energy-Loss Spectroscopy. *Phys. Rev. B* **2000**, *62*, 11126−11133.
(32) Schon, G. ESCA Studies of Ag, Ag_2O and AgO. *Acta Chem. Scand.* **1973**, *27*, 2623−2633.

dx.doi.org/10.1021/la4008526 | *Langmuir* XXXX, XXX, XXX−XXX